Reaction dynamics of molecular hydrogen on silicon surfaces

P. Bratu
Max-Planck-Institut für Quantenoptik, D-85740 Garching, Germany

W. Brenig
Physik-Department, Technische Universität München, D-85747 Garching, Germany

A. Groβ
Fritz-Haber-Institut der Max-Planck-Gesellschaft, D-14195 Berlin-Dahlem, Germany

M. Hartmann and U. Höfer
Max-Planck-Institut für Quantenoptik, D-85740 Garching, Germany

P. Kratzer
Center for Atomic-scale Materials Physics and Physics Department, Technical University of Denmark, DK-2800 Lyngby, Denmark

R. Russ
Physik-Department, Technische Universität München, D-85747 Garching, Germany
(Received 12 October 1995)

Experimental and theoretical results on the dynamics of dissociative adsorption and recombinative desorption of hydrogen on silicon are presented. Using optical second-harmonic generation, extremely small sticking probabilities in the range $10^{-9}-10^{-5}$ could be measured for H_2 and D_2 on Si(111)7×7 and Si(100)2×1. Strong phonon-assisted sticking was observed for gases at 300 K and surface temperatures between 550 K and 1050 K. The absolute values as well as the temperature variation of the adsorption and desorption rates show surprisingly little isotope effect, and they differ only little between the two surfaces. These results indicate that tunneling, molecular vibrations, and the structural details of the surface play only a minor role for the adsorption dynamics. Instead, they appear to be governed by the localized H–Si bonding and Si–Si lattice vibrations. Theoretically, an effective five-dimensional model is presented taking lattice distortion, corrugation, and molecular vibrations into account within the framework of coupled-channel calculations. While the temperature dependence of the sticking is dominated by lattice distortion, the main effect of corrugation is a reduction of the preexponential factor by about one order of magnitude per lateral degree of freedom. Molecular vibrations have practically no effect on the adsorption/desorption dynamics itself, but lead to vibrational heating in desorption with a strong isotope effect. *Ab initio* calculations for the H_2 interaction with the dimers of Si(100)2×1 show properties of the potential surface in qualitative agreement with the model, but its dynamics differs quantitatively from the experimental results. [S0163-1829(96)01732-8]

I. INTRODUCTION

The kinetics and dynamics of hydrogen interaction with silicon surfaces have recently become a topic of extensive experimental[1–16] and theoretical efforts.[17–37] The great interest is, of course, partly due to the importance of H/Si in semiconductor chemistry.[38,39] Equally important, however, hydrogen on silicon is a promising model system for studying general aspects of chemical reactions on covalent surfaces. It may be expected that the localized nature of bonding on semiconductor surfaces gives rise to a reaction behavior that is in many respects qualitatively different from metal surfaces. One particularly far-reaching consequence of the localized nature of H-Si bonds, e.g., are the large diffusion barriers that were observed experimentally for H/Si(111)7×7,[5] which have been predicted theoretically for H/Si(100)2×1.[19,22,28] Also, the finding that the desorption kinetics of H_2 from silicon depend on the details of the surface reconstruction[4,6] is due to the local character of Si–H chemisorption.

The topic of the present paper is another, rather dramatic manifestation of the localized nature of hydrogen interaction with silicon surfaces: the occurrence of strong dynamic lattice distortions in the dissociative adsorption and recombinative desorption of molecular hydrogen on or from Si(111)7×7 and Si(100)2×1. Lattice excitations provide the solution to the so-called ''barrier puzzle'' resulting from recently performed state resolved experiments of hydrogen desorption from silicon surfaces:[9,11,24] It had been known for many years that the room-temperature sticking coefficient of molecular H_2 on silicon surfaces is very low, less than 10^{-6}–10^{-8}.[40–42] This demands the presence of a high adsorption barrier of $V_{ads}>0.5$ eV. However, the energetics of desorbing molecules, in particular the absence of translational heating,[11] indicates the absence of a substantial potential drop during desorption.

Lattice relaxation is frequently associated with

adsorption,[43] and may influence adsorption/desorption barriers even for metal surfaces.[44] In the case of H/Si, theoretical investigations indicate that the diffusion[19,28,32] and desorption barriers[18] decrease substantially when the Si atoms relax. However, a model involving *static* lattice distortion of silicon between the two ''hydrogen-adsorbed'' and ''hydrogen-desorbed'' states, and a corresponding barrier change, would lead to a violation of detailed balance.[11,31] This stimulated our first quantum-mechanical coupled-channel calculation of the adsorption/desorption reaction dynamics of H_2/Si. In the absence of a detailed *ab initio* potential surface (PES), a simple two dimensional model was proposed to study such reactions.[31] It contained—besides the center-of-mass distance of the molecule from the surface—only a single additional coordinate, namely, the amplitude of a ''representative surface oscillator,'' associated with lattice distortions.

The shape of the PES used in Ref. 31 was to a large extent dictated by the existing experimental facts. This implies that during desorption there should be little force exerted on the center-of-mass coordinate in order to avoid translational heating. The high adsorption barrier, needed to explain the low sticking coefficient, has to originate mainly from a strong dependence of the PES on the lattice distortion. A pseudo-three-dimensional (3D) plot is depicted in Fig. 1 of Ref. 31. Such a potential obviously leads to a strong lattice excitation in desorption without significant translational heating. It somehow circumvents Polanyi and Wong's rules[45] for the usual ''curved'' reaction paths which normally produce translational heating together with vibrational heating in exothermic processes. Application of time reversal to such a desorption process then leads to a large sticking coefficient for an excited lattice. Hence such a model predicts strong *phonon-assisted sticking*.

Experimentally, such a strong enhancement of the sticking probability was first observed for H_2 adsorption on Si(111)7×7,[7] and more recently also for Si(100)2×1.[8] In these experiments sticking coefficients of the order of 10^{-9} could be measured with a technique based on optical second-harmonic generation (SHG). In Sec. II of the present paper, we give a more detailed and complete description of these adsorption experiments. We report experiments on the isotope dependence of sticking as well as desorption, and present first results on the coverage dependence of the sticking coefficient on the Si(111)7×7 surface. These results further corroborate our previous conclusions from the observation of phonon-assisted sticking.[7,8] It is the strong lattice distortion in the transition state, as modeled by the PES, that is the dominant mechanism leading to the observed ''asymmetry'' between dissociative adsorption and recombinative desorption. Other effects, such as tunneling or a reaction mediated at static defects, appear to be less important.

Theoretically, we have included more degrees of freedom in the model, i.e., we considered the effect of surface corrugation and molecular vibrations. In Sec. III we show that the main effect of corrugation is a reduction of the sticking coefficient by about one order of magnitude per lateral degree of freedom (depending slightly on temperature). Molecular vibrations have practically no effect on the adsorption/desorption dynamics itself but lead to vibrational heating in desorption with a strong isotope effect. Taken all together, our model allows for a satisfactory description of all currently available experimental results.

Specific microscopic reaction mechanisms will be considered in the last part of Sec. III, and in Sec. IV of the paper. *Ab initio* quantum-dynamical calculations for the interaction of H_2 with the Si–Si dimers of the Si(100)2×1 surface are found to agree qualitatively with the results obtained from the model PES, but seem to underestimate the amount of coupling to the lattice. Possible reasons for the quantitative discrepancies and alternative reaction paths leading to stronger lattice distortions will be discussed.

II. EXPERIMENT

The extremely small sticking coefficients for dissociative adsorption of H_2/Si were measured with optical second-harmonic generation (SHG).[7] For pump wavelengths near 1 μm this technique is very sensitive to the number of Si dangling bonds. It allows the determination of small hydrogen coverages with a sensitivity that exceeds that of most conventional techniques. In the past this high sensitivity has already been exploited for accurate measurements of H_2 desorption kinetics[4,6] and surface diffusion of H/Si.[5] Here we additionally take advantage of the compatibility of SHG with any gas pressure, and measure the H coverage directly during exposure of the surface to a high flux of molecular H_2. This way it is possible to measure sticking coefficients for dissociative adsorption even for surface temperatures that exceed the H_2 desorption temperature. Furthermore, the coverage dependence of the sticking coefficient directly results from these experiments.

A. Experimental conditions

The experiments were carried out in a small UHV chamber with a base pressure of 3×10^{-11} mbar. The Si(100) and Si(111) samples were cut from 10-Ω cm n-doped wafers. They were mounted on a liquid-nitrogen-cooled cryostat and could be heated resistively. Reconstructed Si(111)7×7 and multidomain Si(100)2×1 surfaces were obtained by removing the oxide layer at 1300 K. Surface cleanliness and order were checked by low-energy electron diffraction and Auger electron spectroscopy. The sample temperature T_s was determined by means of a thermocouple glued on the oxidized rear side of the crystal and an infrared pyrometer. The temperature measurement was calibrated at the Si(111)7×7 to 1×1 phase transition.[46] In the temperature range between 500 K and 1100 K, the absolute accuracy is ± 15 K.

For H_2 exposure the UHV chamber was backfilled for 100–1000 s with typically $p=2\times10^{-4}$–5×10^{-3} mbar of purified H_2 or D_2 from a liquid-nitrogen-cooled reservoir. The resulting flux of hydrogen molecules on the surface, $\Phi=p[2\pi m_{H_2}kT_{gas}]^{-1/2}$, varied between 3×10^2 and 2×10^4 ML/s. For some measurements gas pressures up to 10^{-1} mbar and total exposures up to 10^7 L (= 13 mbar s) were used. The gas temperature was $T_{gas}=300$ K. During exposure all filaments in the chamber were turned off and the chamber pressure p was recorded with a spinning rotor gauge (MKS instruments, absolute error $<10\%$). For some experiments that required a constant gas flux, a faster capacitance pressure gauge was additionally employed, and used to

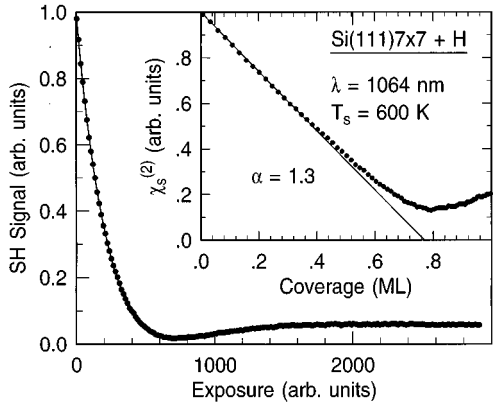

FIG. 1. Coverage dependence of the second-harmonic response of H/Si(111)7×7. The main panel shows the measured SH signal $I(2\omega)\propto|\chi_s^{(2)}|^2$ as a function of exposure to atomic hydrogen. In the inset, the square root of the same data is plotted vs the hydrogen coverage θ. For $\theta<0.4$ ML, the nonlinear susceptibility $\chi_s^{(2)}(\theta)$ of Si(111)7×7 decreases linearly with θ.

regulate a stepper-motor-driven leak valve. For calibration purposes, the samples could also be exposed to atomic hydrogen which was created by dissociation of H_2 at a hot tungsten filament in the vicinity of the sample.

The pump radiation for SHG was supplied by a *Q*-switched Nd:YAG (yttrium aluminum garnet) laser (wavelength 1064 nm, pulse duration 8 ns, repetition rate 10 Hz, beam diameter 6 mm, and peak fluence $\leqslant 50$ mJ/cm^2). It was incident at 45° with respect to the surface normal, and linearly polarized. In the case of the Si(111)7×7 surface, the input and output polarizations were chosen such that the variation of the anisotropic $\chi^{(2)}_{s,\xi\xi\xi}$ component of the second-order nonlinear susceptibility was monitored. For the Si(100)2×1 surface, the polarizer in the output beam path was removed and the input polarization was rotated to optimize the recorded SH intensity. In this case all three isotropic tensor elements ($\chi^{(2)}_{s,\perp\perp\perp}$ $\chi^{(2)}_{s,\perp\parallel\parallel}$ $\chi^{(2)}_{s,\parallel\perp\parallel}$) contribute to the SH response.[47]

B. Calibration of the SH response

The sensitivity of SHG to adsorption of hydrogen on Si(111)7×7 is demonstrated in Fig. 1. Upon exposure of the sample to *atomic* hydrogen, the recorded SH intensity $I(2\omega)\propto|\chi_s^{(2)}|I^2(\omega)$ decreases by a factor of 100, then recovers slightly, and saturates at a value that is 20 times smaller than that of the clean surface. Frequency-dependent measurements show[48] that this behavior arises because the SH response of the clean surface at the pump wavelength of 1064 nm is dominated by resonant optical transitions involving dangling-bond-derived surface states in the bulk band gap. These states are quenched upon hydrogen adsorption,[49] and lead to a strong decrease of $\chi_s^{(2)}$. The SH response of the H-terminated surface originates mainly from nonresonant bulk-derived electronic states. This contribution to $\chi_s^{(2)}$ exhibits a relatively weak coverage dependence, but interferes partially with the dangling-bond-derived response.[48] The plot of the absolute magnitude of $\chi_s^{(2)}$ as a function of H coverage θ reveals a simple linear dependence for $\theta<0.4$ ML,

$$\chi_s^{(2)}(\theta)\simeq\chi_{s,0}^{(2)}(1-\alpha\theta), \tag{1}$$

with $\alpha=1.3$. For this calibration curve the conversion between exposure and absolute coverage was established with the help of a series of temperature-programmed desorption measurements fitted to first-order Langmuir adsorption kinetics $\theta=1-\exp(-c\Phi t)$. The saturation coverage of the Si–H monohydride was identified with the density of dangling bonds of the Si(111)7×7 surface (1 ML $=0.30\times10^{15}$ cm^{-2}). Similar experiments for H/Si(100) have shown up to a 50-fold decrease. For this surface the linear relationship between $\chi_s^{(2)}$ and θ holds up to a coverage of 0.15 ML (1 ML$=0.68\times10^{15}$ cm^{-2}) and the proportionality constant is $\alpha=3.1$.[8]

The calibration curve of Fig. 1 was obtained at the surface temperature $T_s=600$ K. Since the SH response of Si(100) and Si(111) is known to show a non-negligible temperature dependence,[46,48] we should briefly comment on the validity of this calibration at other surface temperatures. From a comparison with adsorption measurements at $T_s<600$ K, and from a modeling of spectroscopic data, we expect a shift of the minimum of $\chi_s^{(2)}(\theta)$ to lower θ with increasing temperature. The estimated variation of the initial slope is 30% for Si(111)7×7 and 50% for Si(100)2×1. In view of the 3–4 orders of magnitude variation of the measured sticking coefficient, this uncertainty of the calibration of $\chi_s^{(2)}(\theta)$ is negligible in the present experiment.

C. Determination of sticking coefficients

In order to determine the sticking probability for dissociative adsorption of H_2, the initially clean Si samples are kept at a certain temperature T_s, and their SH response is recorded as a function of time. At $t=0$ the H_2 or D_2 pressure is increased to a value high enough to cause a detectable decrease of the SH signal due to adsorbed atomic hydrogen or deuterium. Typical data showing the recorded chamber pressure and the H coverage θ determined from the calibrated SH response are plotted in Fig 2. In Fig. 2(a) the sample temperature is too low to cause desorption on the time scale of the experiment. In Figs. 2(b) and 2(c) the desorption rates are appreciable; after the H_2 flux is turned off, the SH response recovers to the value of the clean surface. In the example of Fig. 2(c) the hydrogen coverage reaches an equilibrium of $\theta=0.1$ ML.

Quantitatively, the measured hydrogen coverage $\theta(t)$ is determined by the time-integrated rates of adsorption $k_{\rm ads}$ and desorption $k_{\rm des}$:

$$\theta(t)=\int_0^t[k_{\rm ads}(\theta,T_s,t')-k_{\rm des}(\theta,T_s)]dt'. \tag{2}$$

The adsorption rate

$$k_{\rm ads}(\theta,T_s,t)=\Phi(t)s_0(T_s)f(\theta) \tag{3}$$

is given by the flux $\Phi(t)$ of H_2 molecules derived from the measured pressure $p(t)$, and by the sticking coefficient of the clean surface s_0 multiplied by a factor $f(\theta)$ that describes the coverage dependence of the sticking coefficient.

For most measurements the coverage dependence of the desorption rate $k_{\rm des}(\theta)$ may be deduced directly from the

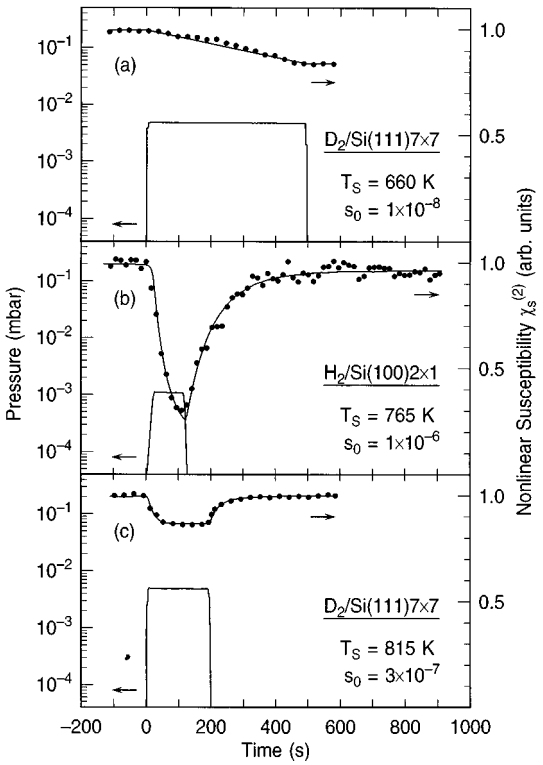

FIG. 2. Typical data for the determination of the sticking coefficient for dissociative adsorption of H_2 and D_2 on Si(111)7×7 and Si(100)2×1 at different surface temperatures. The lines of the lower traces show the recorded gas pressure ($T_{gas}=300$ K) in the UHV chamber. The measured nonlinear susceptibility (dots in the upper traces) is linearly related to the hydrogen coverage. The solid lines through the data points are the result of the numerical fit described in the text.

recovery of the SH signal, measured after the gas flux has been turned off. Since for $\theta \leqslant 0.1$ ML the coverage dependence of the sticking coefficient is weak [$f(\theta)\simeq 1$, compare Sec. II F], the sticking coefficient s_0 is then the only unknown parameter and may be accurately determined by a numerical fit of Eqs. (1)–(3) to the measured time dependence $\chi_s^{(2)}(t)$.

An overview of the surface temperature dependence of the sticking coefficients determined by this procedure for the different surfaces and isotopes will be presented in Sec. II E, together with the results obtained for high surface temperatures. Here we just note that the smallest measurable sticking probabilities were $s_0\simeq 1\times 10^{-9}$ for H_2/Si(111)7×7 at a surface temperature of $T_s=570$ K. These are likely to be the smallest sticking coefficients that have been determined experimentally on an otherwise highly reactive surface. Small amounts of water contamination in the dosing gas ($\ll 1$ ppm) limit the applicability of the technique to even smaller sticking coefficients. Water adsorbs dissociatively on silicon surfaces with a high sticking probability and also quenches the dangling bonds.[8] It may be distinguished unambiguously from the adsorption of H_2 or D_2 by the different desorption kinetics, as discussed in detail in Ref. 8.

D. Desorption rates and sticking coefficients for $T>T_{des}$

For desorption rates $k_{des}>1$ ML/s, the equilibrium between adsorption and desorption $k_{ads}=k_{des}$ is established

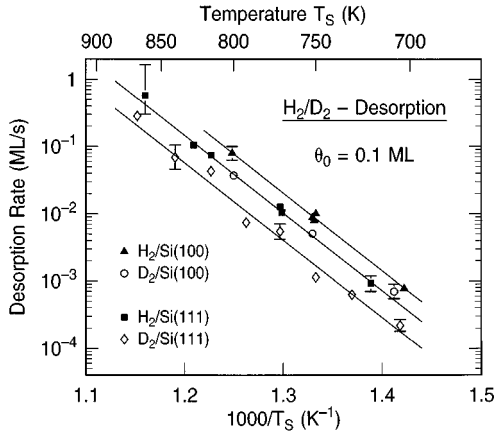

FIG. 3. Desorption rates of H_2 and D_2 from the monohydride states of Si(111)7×7 and Si(100)2×1 as deduced from the recovery of the SH signal after exposure to molecular H_2 or D_2.

faster than the time constant for pressure changes in the present experiment. In these cases, which occur for $T_s>T_{des}\simeq 850$ K, the sticking coefficients may no longer be determined independently from $\theta(t)$. In order to determine the sticking coefficient, we assume a thermally activated desorption process with a desorption rate that may be written in the form

$$k_{des}(\theta,T_s)=\theta^m \nu_{des}^0 \exp(-E_{des}/kT_s). \tag{4}$$

The activation energy E_{des}, the prefactor ν_{des}^0, and the (fractional) reaction order m are obtained from fits of Eq. (4) to the data obtained for $T_s<T_{des}$. With $f(\theta)\equiv 1$ (low coverage approximation), the equilibrium coverage is then given by

$$\theta(t)=\left[\frac{\Phi(t)s_0}{\nu_{des}^0 \exp(-E_{des}/kT_s)}\right]^{1/m}. \tag{5}$$

With respect to the specific form of Eq. (4) we note that previous SHG investigations of hydrogen desorption from Si(111)7×7 have shown that for $\theta<0.15$ ML the coverage dependence of the desorption rate may be parametrized by a reaction order of $m=1.5$.[4] Similar values of $m=1.3$–1.7 were also deduced from the present measurements. In the case of H_2 desorption from Si(100)2×1, $k_{des}(\theta)$ was also found to lie in between first- ($m=1$) and second-order kinetics ($m=2$) for coverages $\theta<0.1$ ML.[6] For simplicity we have also used a fractional reaction order to describe the desorption behavior on this surface. Although the desorption rate is in reality a more complicated function of coverage for both surfaces (in particular, it is not temperature independent), the possible error introduced by the approximation of a fractional reaction order is negligible compared to that resulting from the limited accuracy at which we are able to determine the activation energy for desorption E_{des}.

The Arrhenius plot for the desorption rates of H_2 and D_2 from Si(100)2×1 and Si(111)7×7 is shown in Fig. 3. The different rates were derived from data like those shown in Figs. 2(b) and 2(c), and were normalized to a coverage $\theta=0.1$ ML. The Si(100)2×1 surface exhibits the higher desorption rates than Si(111)7×7. However, the rates differ by less than a factor of 5 between the two surfaces in the inves-

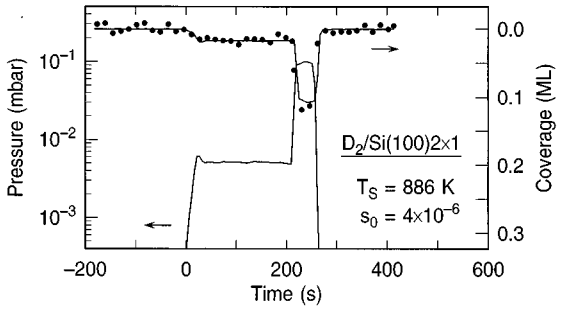

FIG. 4. Data used for the determination of the sticking coefficient of D_2 adsorption on Si(100)2×1 from the equilibrium coverage at a surface temperature of 886 K.

tigated temperature range 700 K $<T_s<$850 K. Likewise, there is no large isotope effect; the rates of D_2 desorption are only 2–3 times smaller than the corresponding rates for H_2. The resulting activation energies for desorption are all between $E_a=2.3$–2.4 eV with an error of 0.2 eV, in good agreement with previous isothermal SHG,[4,6] laser-induced thermal desorption,[2] and temperature-programmed desorption experiments.[41]

The slightly larger uncertainty of E_{des} as compared to our previous results for H_2 desorption from Si(111)7×7 ($E_{\mathrm{des}}=2.40\pm0.1$eV) (Ref. 4) and Si(100)2×1 ($E_{\mathrm{des}}=2.48\pm0.1$ eV) (Ref. 6) simply reflects the limited data set available in the temperature range $700<T_s<850$ K. In principle, once the H_2 flux is turned off, the present experiment is equivalent to the previously employed isothermal desorption scheme. There, atomic hydrogen was adsorbed, and the recovery of the SH signal was observed after the sample temperature was stepped to the desired desorption temperature.[4,6] Here the recovery of the SH signal is initiated by turning the H_2 flux off. Since the latter can be accomplished faster (time constant $<$ 1 s) than changing sample temperatures, the present scheme even allows to access desorption rates as high as $k_{\mathrm{des}}\simeq1$ ML/s compared to $k_{\mathrm{des}}<0.1$ ML/s in the usual isothermal measurements.[1,2,4,6]

With the Arrhenius parameters for the desorption rate, we may now determine the sticking probabilities from the measured equilibrium coverages at $T_s>T_{\mathrm{des}}$. An example for D_2/Si(100)2×1 is shown in Fig. 4. The coverage θ(t) follows the pressure changes almost instantaneously. Its time dependence is well described by Eq. (5). In this particular example the temperature $T_s=886$ K is close to the desorption temperature T_{des}. The error in the determination of the sticking coefficient resulting from the extrapolation of the desorption rate is thus relatively small ($<$50%). For the highest surface temperature of $T_s=1050$ K the desorption rate ($k_{\mathrm{des}}\simeq3\times10^2$ ML/s) already had to be extrapolated by almost three orders of magnitude beyond the measured rates. The large error introduced by this extrapolation currently limits the useful temperature range of our experiments.

E. Surface temperature dependence of sticking

The inferred values for the initial, total sticking coefficient of H_2 and D_2 on Si(100)2×1 and Si(111)7×7 are displayed in Fig. 5 as a function of the inverse surface temperature. The smallest sticking coefficients could be observed for H_2/Si(111)7×7. They are on the order of 10^{-9} for a surface temperature of 550–600 K. The sticking coefficient s_0 increases by almost four orders of magnitudes to 5×10^{-6} when the temperature is raised to 1050 K. The two symbols used to mark the sticking coefficients for H_2/Si(111)7×7 denote different experimental conditions. The full squares indicate data already published in Ref. 7; full diamonds are data obtained with samples from different Si wafers. The good agreement demonstrates the high degree of reproducibility of our experimental procedure to determine such small sticking coefficients.

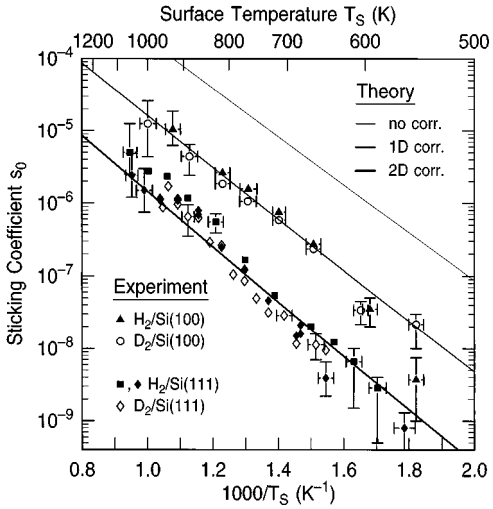

FIG. 5. Initial sticking coefficient of thermal H_2 and D_2 gases at $T_{\mathrm{gas}}=300$ K on Si(111)7×7 and Si(100)2×1 surfaces as a function of their inverse temperature. The experimental values are denoted by symbols; lines are results of theoretical calculations described in Sec. III (thin upper line: basic 2D model without corrugation; intermediate line: 3D calculation including corrugation in one dimension; thick lower line: extrapolation to two-dimensional corrugation).

The open diamonds in Fig. 5 denote the values of s_0 for D_2/Si(111)7×7. Both the absolute values and the temperature dependence of the sticking coefficient exhibit only a very weak isotope effect. An analogous behavior was previously observed for the sticking of H_2 and D_2 on Si(100)2×1.[8] These data are included in Fig. 5 for the purpose of comparison with the theoretical results of Sec. III. On Si(100) the overall sticking coefficients are higher by a factor of 2–10 than on the Si(111) surface. Their temperature dependence is slightly weaker, but still quite dramatic, with s_0 increasing by three orders of magnitude in the temperature range 550–1000 K.

The small sticking probabilities that we were able to determine quantitatively in the present experiments are in agreement with the lower limits given earlier in the literature. In 1959, Law[40] reported that the exposure of single-crystal Si filaments to large fluxes of molecular hydrogen leads only to weak flash desorption signals. Already from these old data one may deduce that the room-temperature sticking coefficient on the terraces of the Si filaments is less than 10^{-8}. Later, Schulze and Henzler[41] gave upper bounds of $s_0<10^{-6}$ for the sticking of H_2 on Si(111)7×7, and Liehr *et al.*[42] found $s_0<10^{-8}$ for H_2/Si(100)2×1. Much higher sticking coefficients, on the order of 10^{-5}, were recently

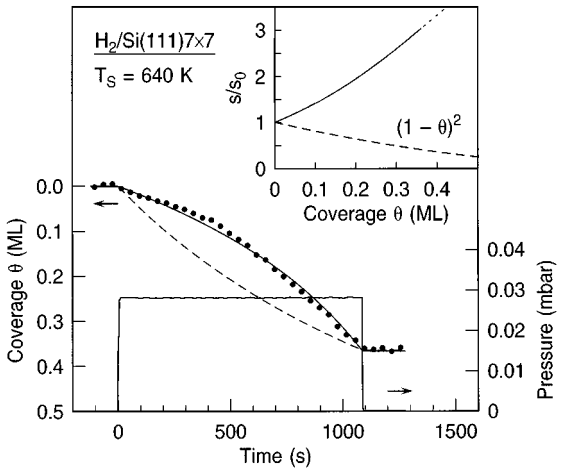

FIG. 6. Coverage dependence of the sticking coefficient of H_2 on Si(111)7×7 at a surface temperature of $T_s = 640$ K.

reported for D_2/Si(100)2×1 by Kolasinski *et al.*,[12] based on a molecular-beam experiment with nozzle temperatures between 300 and 1000 K. The effective Arrhenius energy describing the surface temperature dependence of their sticking coefficient in the range 300 K $< T_s <$ 650 K is less than 0.1 eV. This rather weak dependence of the sticking coefficient on surface temperature stands in marked contrast to results of the present work ($E_a = 0.7$ eV). Although the reasons for these discrepancies are currently still unclear, it should be kept in mind that the beam experiment lacked the sensitivity to measure sticking coefficients below 5×10^{-6}.[12] For a more detailed comparison of our Si(100) data with the measurements of Kolasinski *et al.*, see Ref. 8.

The strong effect of the surface temperature on the sticking probability that we observe shows, independent of any particular theoretical model, that substrate excitations must play a decisive role in the reaction dynamics of H_2 with silicon surfaces. The behavior may be approximated by an Arrhenius law, $s_0 = A\exp(-E_a/kT_s)$, with activation energies ranging between $E_a = 0.7$ eV for D_2/Si(100)2×1 and $E_a = 0.9$ eV for D_2/Si(111)7×7. The prefactors are of the order $A \simeq 10^{-2} - 10^{-1}$. Fits of some of these data to Arrhenius law have been shown in Refs. 7 and 8. In Fig. 5 we directly compare the data with the results of the theoretical calculations described in Sec. III. The thin solid line is the temperature dependence calculated from the basic two-dimensional model without corrugation. For the thick solid lines corrugation in one and two dimensions was taken into account in the calculation. Please note that the theoretical curves are *not fitted* to the experimental data. The coincidence of the calculation involving 1D/2D corrugation with the experimental data for Si(100)/Si(111) is to some extent accidental. A more detailed comparison of experimental and theoretical sticking probabilities will be given in Sec. III A.

F. Coverage dependence of sticking

For comparison with theory, the most interesting quantity is the sticking coefficient of the clean surface. For this reason, all values plotted in Fig. 5 were extracted from data with a total hydrogen coverage $\theta \leqslant 0.1$ ML. Apart from this initial sticking coefficient $s_0 = s(\theta = 0)$, we have also performed some experiments on the coverage dependence $s(\theta) = s_0 f(\theta)$. For surface temperatures $T_s \ll T_{\rm des}$ our techniques enable us to perform such measurements very accurately, simply by extending them to higher exposures. An example for H_2/Si(111)7×7 is shown in Fig. 6. The data clearly show that the slope $-d\theta/dt$, which is proportional to the sticking coefficient $s(\theta)$, increases as a function of exposure time and thus as a function of coverage.

The observed behavior is in contrast to the expected effect from site blocking which in this coverage range should already result in a noticeable decrease of the sticking coefficient. A comparison with a fit to $f(\theta) = (1-\theta)^2$ is shown as a dashed line in Fig. 6. Obviously the data are also incompatible with a simple defect-mediated adsorption process. If the low sticking coefficients were primarily caused by a low concentration of available adsorption sites then the sticking coefficient should decrease even more strongly with coverage, in complete contrast to the observed increase. The shape of measured θ(t) also deviates significantly from a linear increase of θ [$f(\theta) = 1$], which could be expected approximately for precursor mediated adsorption in the coverage range $\theta < 0.5$ ML.

The increase of the sticking coefficient with coverage is likely to be caused by a slight decrease of the adsorption barrier for sites in the vicinity of adsorbed hydrogen. This effect should depend in general on the specific local coordination of reacted and unreacted sites, and is thus difficult to model quantitatively. To gain some insight, we have made a rather crude model, and simply assume an average adsorption barrier that exhibits a weak negative coverage dependence

$$E_a = E_{a,0}(1-\beta\theta). \tag{6}$$

If we include the usual site blocking, then the sticking coefficient $s = A\exp(-E_a/kT)$ takes the simple form

$$s(\theta) = (1-\theta)^2 s_0^{(1-\beta\theta)}. \tag{7}$$

Good fits of this functional form to the experimental data were obtained for $\beta \simeq 0.25$. The inset of Fig. 6 shows the coverage dependence s(θ) resulting from the best fit of Eq. (7) to the measured θ(t). The fivefold increase of the sticking coefficient, as compared to the $(1-\theta)^2$ behavior, corresponds roughly to a 10% reduction of the adsorption barrier. Such a small reduction of the adsorption barrier could be caused by several mechanisms: For example, the weakening of the adatom backbonds of Si(111)7×7,[50] which is likely to occur upon hydrogen adsorption, could decrease the amount of lattice distortion required to form the transition state. In addition, also purely electronic effects, such as band flattening or redistribution of charge between the dangling bonds of Si(111)7×7, could reduce the adsorption barrier with increasing hydrogen coverage. Which of these two effects is the more important could be decided by investigating the coverage dependence for different gas and surface temperatures. For the Si(100)2×1 surface the coverage dependence of the sticking coefficient was found to be much weaker than for Si(111)7×7.

III. THEORY

In this section we intend to show that all experimental observations can be described in a coherent way as the result of the dynamics on a suitably chosen potential-energy surface. The most important degree of freedom, apart from the reaction coordinate s (Refs. 51–54) itself, is the motion of the substrate lattice during the adsorption/desorption process. We describe this part of the dynamics by a representative coordinate x. Additionally we will take the molecular vibrations (coordinate r) and the surface corrugation (coordinate $\vec{y}$) into account. In total our model covers five degrees of freedom.

We assume that the potential can be written as a sum of the following four terms:

$$V(x,\vec{y},r;s)=V_{\text{trans}}(s)+V_{\text{phon}}(x;s)+V_{\text{corr}}(\vec{y};s)+V_{\text{vib}}(r;s). \tag{8}$$

The first term $V_{\text{trans}}(s)$ then gives the value along the *minimum* of the multidimensional potential with respect to the coordinates orthogonal to s, i.e., along the line of steepest descent of the PES. We have chosen the following general parametrization:

$$V_{\text{trans}}(s)=(V_{\text{des}}-V_{\text{ad}})\frac{\tanh(\lambda s)-1}{2} + \frac{1}{4}(V_{\text{des}}+V_{\text{ad}}+2\sqrt{V_{\text{des}}V_{\text{ad}}})\frac{1}{\cosh^2(\lambda s)}, \tag{9}$$

with $V_{\text{ad}}=0.7$ eV for H_2, a desorption barrier of $V_{\text{des}}=2.5$ eV, and a potential decay length of $\lambda=2.7$ Å^{-1}. The desorption barrier V_{des} is known from experiment (Sec. II D, Refs. 2, 4, and 6) and λ was estimated. The results are not very sensitive to the latter two quantities, but only to the adsorption barrier V_{ad}, which thus is the single essential parameter.

The second term $V_{\text{phon}}(x;s)$ describes the coupling of adsorption and desorption to the substrate;

$$V_{\text{phon}}(x;s)=\tfrac{1}{2}\hbar\omega_{\text{phon}}(s) \times d(1-\exp\{-\alpha\gamma_{\text{phon}}(s)[x+\Delta x(s)]\})^2. \tag{10}$$

The phonon potential depth d is given by the square root of the number of bound states which we choose to be $d^2=52$ for the model PES. The inverse oscillator length is $\gamma_{\text{phon}}(s)=\sqrt{M^*\omega_{\text{phon}}(s)/\hbar}$, with the frequency $\hbar\omega_{\text{phon}}(s)=E_1(s)-E_0(s)$ as the quantum of the first excited state, and thus $\alpha=\sqrt{d}/(d-1)$. We estimate the effective phonon mass M^* to be the mass of one single Si atom, and for the frequency we use $\hbar\omega_{\text{phon, clean}}=45$ meV. The latter is a mean value of several optical modes.[34,55,56]

The last two terms allow us to include the effect of a lateral one- or two-dimensional corrugation and the molecular vibrations. At present our model does not include orientational effects of the hydrogen molecule. This means first of all that we cannot describe the rotational cooling observed experimentally.[9] Concerning the temperature dependence of sticking coefficients, we expect mainly a further reduction of the preexponential.

For the later discussion of specific microscopic mechanisms, we emphasize at this point that the obtained results are determined mainly by the choice of the adsorption barrier V_{ad} and the displacement Δx. The detailed shape of the PES before and far after the transition state is of little importance for the adsorption/desorption dynamics. In particular, it is not necessary that the lattice distortion be the result of a static Si displacement in the adsorbed state as we assume in this section for the purposes of explicit calculation. A transient lattice distortion in the transition state would result in an almost identical dynamical behavior.

The organization of this section follows the different terms of Eq. (8). The results of the model including only the first two terms were reported in Ref. 31. We extend these calculations to three dimensions with different degrees of freedom included: In Sec. III A we additionally consider a 1D surface corrugation. In Sec. III B we additionally study the vibrational dynamics of the molecules.

The experimental results are very similar for the Si(111) and Si(100) surfaces. This indicates that the basic physics is the same on both surfaces, and that the model considered here can be used to describe the adsorption and desorption dynamics in a general way. We will consider a specific microscopic mechanism in Sec. III C, and compare the dynamical properties of an *ab initio* PES for the interaction of H_2 with the dimers of the Si(100)2×1 surface with that of the model PES.

A. Effect of surface corrugation

The dominant effect of surface corrugation for molecules impinging under normal incidence on a surface is a reduction of the sticking coefficient.[57,58] The variation of the barrier height across the surface leads to a ''keyhole effect,'' i.e., a more or less geometrical decrease of the effective surface area available for sticking which is independent of the energy at low energies. From our investigations of the situation for H_2/Cu (Ref. 57) we know that this effect can cause a reduction of about two orders of magnitude. For non-normal incidence the role of surface corrugation is more complex. The additional parallel momentum can lead to an enhancement or a suppression of the sticking coefficient, depending on the type of corrugation and the energy regime.[58,59]

In this calculation we assume an energetic corrugation of the potential where only the height but not the position of the barrier is varied along the surface. The corresponding term in Eq. (8) is

$$V_{\text{corr}}(\vec{y};s)=V_0\frac{1}{4\cosh^2(\lambda_{\text{corr}}s)}\left\{\left[1-\cos\left(\frac{2\pi}{a}y_1\right)\right]+\left[1-\cos\left(\frac{2\pi}{a}y_2\right)\right]\right\}. \tag{11}$$

Here $\vec{y}$ means the center of mass coordinate parallel to the surface with a periodicity length of $a=2.4$ Å taken from the Si lattice spacing. The range of the corrugation perpendicular to the surface was taken to be $\lambda_{\text{corr}}=2.2$ Å^{-1}, which we estimated from our experience with H_2/Cu.[57] The height

V_0 is determined so as to lead to a lateral H_2 frequency of $\omega = 0.06$ eV, in agreement with electron-energy-loss spectroscopy experiments.[60,61] This leads to the reasonable value of $V_0 = 0.25$ eV.

We will present a 3D calculation where we consider a 1D surface corrugation in addition to the basic model.[31] This reduces the absolute value of the sticking coefficient by about one order of magnitude. Another order of magnitude may be expected for a 2D corrugation, which in principal would have to be considered. However, one needs about 20 channels (reciprocal-lattice vectors) to represent the scattering states in the lateral direction in these calculations, in addition to about 20 channels for the lattice vibrations. Thus a 3D model already requires 400 channels. A 4D model with 2D corrugation would require 8000 channels, and presently leads to problems with computing time and memory space.

In Fig. 5 the calculated sticking coefficient for the flat and the corrugated surface are shown in comparison to experimental results. Indeed, the inclusion of 1D surface corrugation leads to a reduction of the sticking coefficient by one order of magnitude. The sticking coefficients have been determined for a gas of hydrogen molecules with gas temperature $T_{\mathrm{gas}} = 300$ K. This means that molecules contribute to the sticking probability hitting the surface under all possible angles. A more detailed analysis reveals that for molecules under normal incidence the sticking probability is only reduced by a factor of 3. The additional reduction of the sticking coefficient of the hydrogen gas comes from the fact that for an energetically corrugated surface the sticking probability of the molecules which hit the surface under non-normal incidence is suppressed by their additional parallel momentum.[58,59] In a more realistic description not only the variation of the barrier height but also the variation of the barrier position with y_1 and y_2, the so-called geometric corrugation,[59] should be taken into account; the situation then becomes more complex.[58,59] The effect of full 2D corrugation is estimated in Fig. 5 by taking into account a further reduction factor corresponding to the reduction between the flat surface and the 1D corrugated surface.

In addition to the preexponential, the effective barrier is also influenced by surface corrugation. First of all, there is a contribution from the zero point energy (0.03 eV per lateral degree of freedom), and a further increase by about 0.05 eV due to thermal averaging of the potential (11). All together the two lateral degrees of freedom increase the barrier of the 2D model by about 0.16 eV. To obtain agreement with experiment, this has to be subtracted from the minimum-energy barrier.

In our calculations the rotational degrees of freedom of the hydrogen molecule are not considered. Since the barrier height also depends on the orientation of the molecule, taking these degrees of freedom into account would probably lower the sticking coefficient even more. On the other hand, the effective activation energy will also be increased because the corrugation in the polar and azimuthal coordinates of the H_2 molecule will have effects similar to the lateral surface corrugation. Thus, finally, a smaller minimum barrier could be chosen to represent the experimental data. This may bring the barrier of the model closer to the barrier found in *ab initio* calculations.

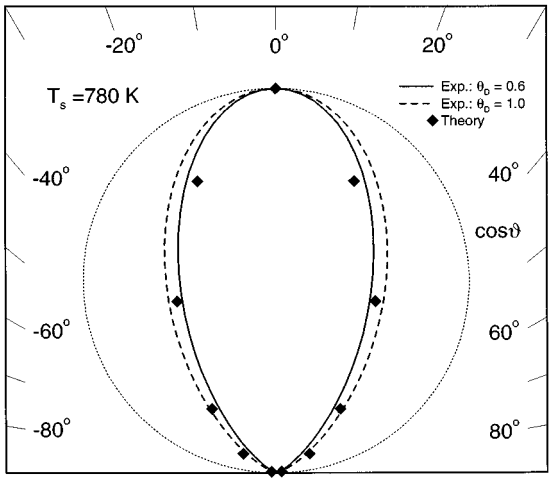

FIG. 7. Polar plot of the angular distribution of hydrogen molecules desorbing from Si(100). The experimental data for deuterium desorption have been determined for coverages of $\theta_D = 0.6$ (solid line) and $\theta_D = 1.0$ (dashed line) (Ref. 14). The theoretical results are indicated by diamonds. The $\cos\theta$ distribution is also shown as the dotted circle for comparison.

Desorbing molecules mainly propagate along paths which pass the barrier region close to the minimum-energy barrier position.[58] In order to check whether our model potential properly describes the experimental situation in the vicinity of the minimum-energy path, we have also calculated the angular distribution of desorbing molecules. Experimentally it is not $\propto \cos\vartheta$, where ϑ is the angle from the surface normal, as one would expect from a thermal distribution, but forward-peaked $\propto \cos^n\vartheta$, with $3.9 \leqslant n \leqslant 5.2$ depending on the surface coverage.[14] Figure 7 shows that there is a rather good agreement between theory and experiment. We also tested a surface corrugation corresponding to a lateral H_2 frequency of $\omega_s = 0.10$ eV which gave a narrower angular distribution in desorption than observed experimentally. Thus our dynamical simulation puts some constraints on the shape of realistic potential-energy surfaces.

The noncosine angular distribution in desorption is, indeed, an indication that the desorbing molecules do not really obey a thermal distribution. Even the *energy* distribution in our model is not really thermal: it appears to be approximately $\propto E \exp(-E/kT_s)$ already in the original 2D model, where a Boltzmann distribution actually should behave like $\propto \exp(-E/kT_s)$.

Our interpretation of this result is that the energy distribution—at least at low energies—is essentially a reflection of the Franck-Condon factors of the lattice vibrational energy distributions in the distorted and undistorted lattice, and *not* of an actual thermal equilibrium with the lattice. This is corroborated by the fact that the average kinetic energy of the desorbing particles at low energies increases less than kT_s (see Fig. 8) with increasing surface temperature as already mentioned in Ref. 31. In addition, Fig. 8 shows that by including surface corrugation the mean kinetic energy normal to the surface is slightly increased as compared to the noncorrugated surface, due to the variation in barrier height,

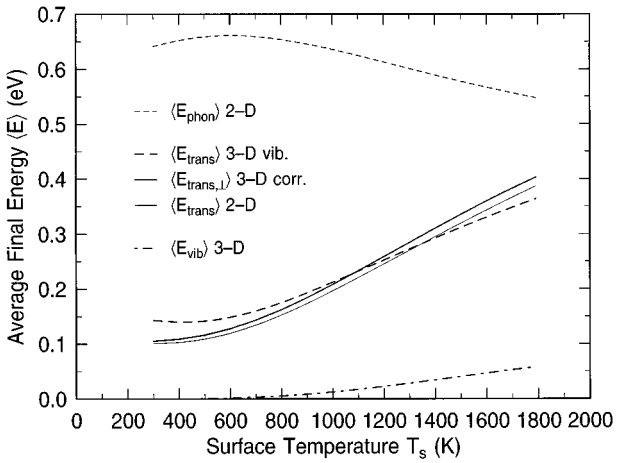

FIG. 8. Average final energies after desorption of translation $\langle E_{\mathrm{trans}}\rangle$ as well as surface $\langle E_{\mathrm{phon}}\rangle$ and molecular excitations $\langle E_{\mathrm{vib}}\rangle$ as a function of surface temperature. Results of the 2D as well as the two 3D calculations are shown. The ground-state energies for the average phonon and vibrational energies have been subtracted.

except for very low surface temperatures when almost all desorbing molecules follow a path through the minimum barrier position.

B. Molecular vibration dynamics

The molecular vibration dynamics leaves the adsorption/desorption dynamics of the model calculations presented above essentially unchanged. This is obvious from the small amount of energy transferred into the intramolecular degree of freedom. Although the population of the first excited state of the desorbing molecule at a surface temperature of 780 K is about a factor of 20 higher than for thermally equilibrated molecules, the difference in average vibrational energy is merely about 6 meV for H_2, 10 meV for HD, and 25 meV for D_2.

Nevertheless, the vibrational dynamics of the molecules, including its isotope effect, is interesting in itself. In this section we will present the study of a 3D model, considering the molecular vibrational degree of freedom in addition to the molecular translation and surface phonons which were already discussed above and in an earlier publication.[31] We apply the INTRA-LORE iteration scheme of the coupled-channel equations described in Refs. 62 and 53.

The vibrational dynamics of the molecule is included by considering a stretching of the intramolecular bond length, leading to an elbowlike curved reaction path.[51] In order to apply the coupled-channel method, one has to transform to a locally orthogonal coordinate system spanned by the reaction path coordinate s and the oscillator coordinate r.[63] Thus molecular vibration is taken into account by adding a harmonic potential in Eq. (8):

$$V_{\mathrm{vib}}(r;s)=\tfrac{1}{2}\hbar\omega_{\mathrm{vib}}(s)(\gamma_{\mathrm{vib}}(s)r)^2. \tag{12}$$

The inverse oscillator length is $\gamma_{\mathrm{vib}}(s)=\sqrt{\mu\omega_{\mathrm{vib}}(s)/\hbar}$, with μ the reduced mass of the hydrogen molecule and $\hbar\omega_{\mathrm{vib}}(s)$ the frequency of the molecular vibration.

Vibrational dynamics has been the subject of various investigations of hydrogen desorbing from metal surfaces.[64,52,65] The vibrational heating is well understood, and the properties of the PES are well known. Although the bonding of hydrogen to the silicon surface is quite different from metal surfaces, one can expect that the PES describing the vibrational dynamics at semiconductor surfaces is similar apart from some details. The value of the curvature as well as a reduction of the vibrational frequency to about 50% for the adsorbed hydrogen are taken from the *ab initio* calculations (see Sec. III C).

Despite all similarities to metal surfaces, the energy distribution on the different degrees of freedom for this PES is quite different: The coupling to lattice distortions is strong, and thus almost all of the potential drop is transferred to surface phonons while only a small portion ends up as additional molecular vibration. This is documented by Fig. 8, where the state-averaged final energies (above the ground-state energy) of surface phonons, molecular translation, and molecular vibration are plotted as a function of surface temperature. The average phonon energy is dominant, and remains nearly constant at 0.65 eV. The translational part increases with surface temperature due to the broadening of the wave function, that makes it impossible to find an *optimal* way through the PES. The average vibrational energy is negligible on the whole temperature scale, although it rises for very high surface temperatures. The effects of taking molecular vibrations additionally into account is exhibited by comparison with the curves for the 2D calculation shown as hairlines in Fig. 8. Though the average phonon energy is slightly reduced by a constant amount, the additional degree of freedom takes its energy from the translational part, i.e., it causes a reduction of translational heating at high surface temperatures.

The vibrational quantum of H_2 molecules in the gas phase is $\omega_{\mathrm{vib}}=516$ meV, and for HD and D_2 it is $\omega_{\mathrm{vib}}=450$ meV and $\omega_{\mathrm{vib}}=371$ meV, respectively. The vibrational population ratios we find at a surface temperature of $T_s=780$ K are $P_1/P_0=0.012$, 0.022, and 0.052 for H_2, HD, and D_2. The ratio for the heavier molecules is larger due to their smaller vibrational quantum. These results are in good agreement with the vibrational state resolved measurements of Kolasinski and co-workers.[9]

Another consequence of the different vibrational frequencies, together with the reduction of these values for the adsorbed hydrogen, is a difference in the effective potential barrier for the various isotopes. As D_2 has the lowest frequency, it consequently has the highest effective adsorption barrier. This results in the following: (i) There is a smaller sticking coefficient in adsorption. For a thermal gas at 300 K for which the calculated results are shown in Fig. 5, we find a difference in the sticking coefficient of a factor 1.5–2. This is also supported experimentally though less pronounced. (ii) It causes a larger translational heating in desorption. The translational energy distribution is approximately Maxwellian and nearly in thermal equilibrium with the surface. For a surface temperature of $T_s=780$ K we calculated a mean translational energy of $\langle E_{\mathrm{trans}}\rangle=97$ meV for H_2 and $\langle E_{\mathrm{trans}}\rangle=106$ meV for D_2. Unfortunately, up to now, experimental measurements of the translational energy distribution were only done for D_2 and therefore experimental knowl-

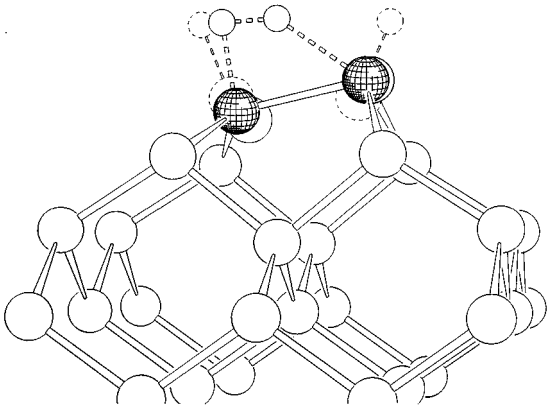

FIG. 9. Ball-and-stick model of H_2 interaction with the buckled dimer of Si(100)2×1, resulting from density-functional calculations (Ref. 33); small balls indicate H atoms, while the Si lattice is shown as large white balls. Before the reaction the Si dimer is tilted by 18 °. Since the ''down'' atom is less charged and thus less repulsive toward H_2 than the ''up'' atom, dissociation starts at the ''down'' atom. In the transition state the H–H distance is increased from 0.8 to 1 Å and the ''down'' atom exhibits an upwards displacement of roughly 0.3 Å (dark balls). At the end of the reaction the dimer is symmetric with two H atoms adsorbed (dashed balls). The total vertical Si displacements during the reaction are 0.5 Å for the ''down'' atom and 0.2 Å for the ''up'' atom.

edge about that consequence of the isotopic effect is not yet available. At least the thermal Maxwellian distribution is experimentally supported.[11]

Another isotopic effect is caused by the stronger coupling for deuterium due to its heavier mass. As shown above in Fig. 5 for the sticking coefficient of a thermal gas, this results in a higher value for the Arrhenius energy for D_2 compared with H_2. In the desorption reaction it leads to an additional increase of the translational energy for the heavier molecules. An isotope effect based on quantum-mechanical tunneling is negligible because of the large barrier width.

C. Comparison of model and *ab initio* quantum dynamics for H_2/Si(100)2×1

In Sec. III we *proposed* a model, and we showed that it describes the experimental results correctly if its parameters are chosen appropriately. The dominant effect on the dynamics comes from strong lattice distortion in the transition state of H_2/Si as compared to the clean surface. We have not specified the microscopic nature of the relaxation process denoted by the coordinate x in Eq. (8). It could simply be a Si–Si bond length or the distance of the reactive silicon atom to the underlying Si layer. In a more general way, this coordinate could also describe long-ranged bulk or even nonadiabatic electronic relaxation processes. It is the exact nature of the coordinate x that is currently the missing link in order to arrive at a completely satisfactory microscopic description.

Recently, there have been several attempts to establish a microscopic picture of the substrate relaxations for hydrogen on Si(100)2×1 by performing *ab initio* calculations.[30,33,35] It has been proposed that the most important process of hydrogen interaction with Si(100)2×1 is the interaction of both hydrogen atoms with a single Si–Si dimer on the Si(100)2×1 surface.[2,3,6,23] Together with the prepairing of the hydrogen atoms on these dimers, this mechanism provides the most natural explanation for the observed first-order desorption kinetics. The asymmetry between dissociative adsorption and recombinative desorption arises because the silicon dimers are found to be horizontally oriented when hydrogen is adsorbed,[3,66] whereas they are buckled on the clean surface.[67–69] Since the buckling is accompanied by charge transfer within the dimer and a rehybridization of orbitals in the two silicon atoms,[68,70] there is a notable dependence of the H_2 adsorption barrier on the buckling angle.[33,35] The minimum reaction path resulting from the calculations of Ref. 33 is depicted in Fig. 9. It very clearly shows the displacement of two silicon atoms in the course of the reaction.

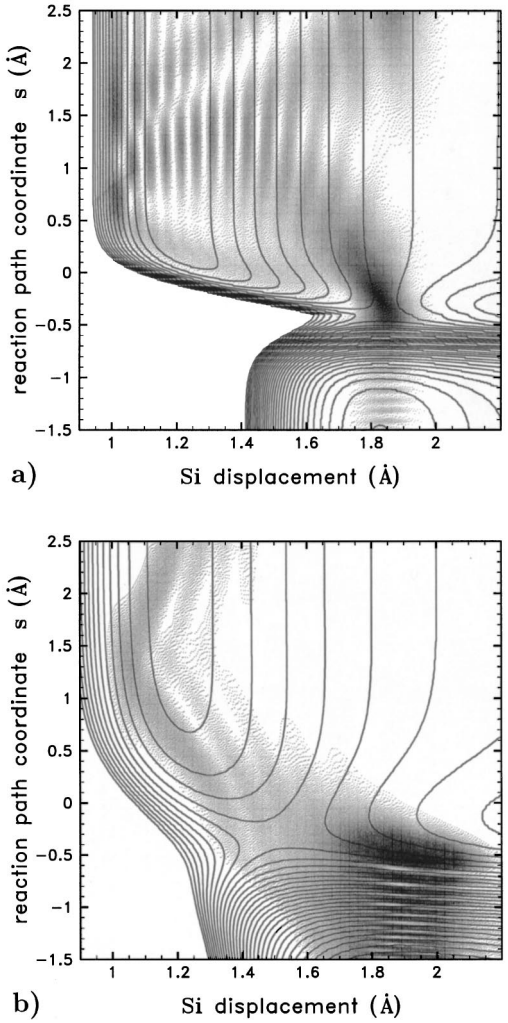

FIG. 10. Contour plots for H_2 of the projection of (a) model PES and (b) *ab initio* PES on the surface degree of freedom. The lattice distortion of the *ab initio* PES varies more slowly with the reaction path as compared to the model and only roughly 1/3 of the ~0.6 Å shift takes place on the gas phase side of the barrier. We include dithered plots of desorption wave functions at $T_s = 1000$ K (see discussion in text). The spacing between the contours is 100 meV.

In a qualitative way the different dynamics of the parameter-free PES based on density-functional theory[33,34] and the model PES discussed above may be recognized from Fig. 10. This displays the projection of the PES on the pho-

non degree of freedom x together with the absolute square of the desorption wave function at $T_s = 1000$ K. In the case of the *ab initio* PES, x is the distance of the lower dimer atom to the underlying Si layer. Since the bond length of the Si–Si dimers change only moderately upon hydrogen adsorption (from 2.32 Å on the clean surface to 2.44 Å in the monohydride,[33]) representing the coupling to the lattice by this coordinate is expected to be a good approximation. The desorption process essentially starts from the ground state of the lattice oscillator and a translational energy of 1000 K. The large oscillation amplitude for the model PES [Fig. 10 (a)] indicates that the potential drop is practically all converted into lattice energy. In the corresponding results of the *ab initio* PES [Fig. 10 (b)], a strong lattice oscillation is found as well, but a substantial portion of the potential drop is converted into translational energy. This is due to the quantitative differences in the similarly shaped potentials. Although the total displacement between the asymptotic states is comparable, $\Delta x \simeq 0.6$ Å in both cases, the barrier of the *ab initio* PES occurs *late in desorption*. Therefore, the dynamically important shift of the barrier position in the x coordinate, measured relative to gas phase H_2 and the clean surface, is only $\Delta x \simeq 0.3$ Å, considerably less than in the model PES. Moreover, the range parameters λ in the two potential surfaces are different by a factor of about 2. The effective minimum barrier heights including zero-point corrections are 0.38 eV for H_2 and 0.41 eV for D_2. All this causes a substantial force along the translational coordinate, leading to a strongly heated translational energy distribution after desorption.

Quantitatively, we find a mean translational energy of $\langle E_{\text{trans}} \rangle = 308$ meV for H_2 and $\langle E_{\text{trans}} \rangle = 336$ meV for D_2 at $T_s = 780$ K. In contrast, the model PES yields 76 and 85 meV, in agreement with experiment.[11] The dependence of the sticking probability on surface temperature resulting from the *ab initio* PES is not as pronounced as the corresponding one for the model PES, indicating a lack in coupling strength. The Arrhenius energy is only about 250 meV for the sticking of a thermal gas of H_2 at 300 K, whereas $E_{\text{Arr}} \approx 650$ meV in the case of the model PES. Due to the lower adsorption barrier the absolute value of the sticking coefficient at a common surface temperature is 10–100 times higher for the *ab initio* model than the results of corresponding calculations in Sec. III A. In contrast to that, the molecular degree of freedom is quite well described, as can be seen from the desorption population ratio P_1/P_0 of the final vibrational states. The vibrational heating found in the experiment[9] is reproduced. In detail we obtain $P_1/P_0 = 0.007$ for H_2 and $P_1/P_0 = 0.074$ for D_2 at a surface temperature of $T_s = 780$ K, which is within the experimental error bars.

The PES we obtained from density-functional theory calculations thus clearly shows that the substrate plays an important role in the dynamics of the reaction. Besides the experimental results this gives additional support for the qualitative correctness of our model. Furthermore, the vibrational population ratio, i.e., the molecular degree of freedom, is also quantitatively well described. Therefore, we have reason to believe that the curvature of the reaction path, which we took over for the model PES, is reliable.

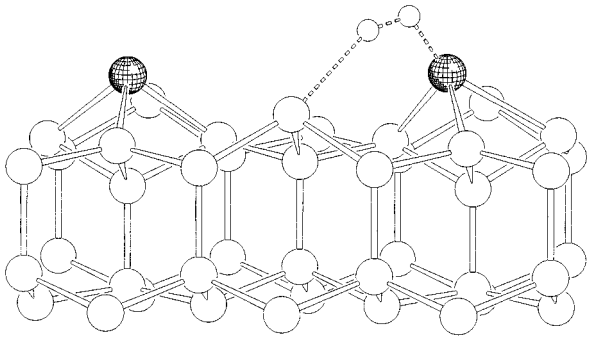

FIG. 11. Possible transition state of H_2 interaction with the 7×7-reconstructed Si(111) surface. The reacting Si adatom (right dark ball) is significantly displaced from its equilibrium threefold coordinated site (left dark ball).

Nevertheless, the *ab initio* PES does not give quantitatively satisfying results for the surface effects. One possible reason for the discrepancies could be due to the fact that we have only considered the supposedly most important phonon mode, and underestimated the coupling to the surface degrees of freedom. In addition, long-range interactions, which are not taken into account, could be important. Probably even more important, the derivation of potential-energy surfaces from density-functional calculations, and in particular the use of gradient-corrected density functionals, is a newly developing field, and little experience is yet available to really check the degree of accuracy of these results.[71] The existence of several geometrically distinct transition states, however, requires an accurate knowledge of the relative barrier heights to decide which of them is the dominant one. The symmetric transition state, for instance, was found to be only slightly higher in energy than the asymmetric one, and involves a stronger effective lattice distortion. Therefore adsorption through this transition state leads to a somewhat stronger coupling to the lattice.[72]

IV. DISCUSSION OF MICROSCOPIC MECHANISMS

The microscopic reaction mechanism considered in Sec. III C is not the only one that is conceivable. In fact, a number of models have been proposed based on *ab initio* theoretical work for H_2 adsorption and desorption on Si(100)2×1.[17–37] Unfortunately, the results of the calculations are partially contradictory, and, despite the enormous efforts, no detailed picture has been established up to now. In this section we would like to discuss some of these models in light of the experimental and theoretical results presented above. In this discussion we will implicitly assume that adsorption and desorption occur via the same mechanism. Peculiar nonequilibrium desorption mechanisms will not be considered.

Although no serious theoretical attempts have yet been devoted to H_2 interaction with Si(111)7×7 because of its large unit cell, from a qualitative point of view the reaction mechanism currently appears to be even clearer for the Si(111) than for the Si(100) surface. The basic building blocks of the 7×7 reconstruction are fairly simple and well understood.[50] Moreover, the coverage dependence of sticking reported in Sec. II F indicates that defects should be unimportant. The reaction of H_2 with Si(111)7×7 should thus

be dominated by the rest atom and adatom dangling bonds (db's) on the terraces. Since the restatom db's are doubly occupied, whereas the adatom db's are only partially filled,[49] hydrogen dissociation (and recombination) is likely to have an asymmetry toward the adatoms. With 4 Å, the closest distance between a restatom and an adatom is large compared to the Si–H bond length of 1.6 Å and the H–H distance of 0.8 Å. Therefore, substantial distortion of the adatom bonding in the transition state, as shown schematically in Fig. 11, is likely to occur. Such a picture of distorted adatoms is supported by the recent work of Vittadini and Selloni,[73] who calculated that the minimum-energy path for hydrogen diffusion from the adatoms to the rest atoms involves substantial bond weakening of one adatom backbond. It is further supported by the fact that the activation energy for phonon-assisted sticking of 0.8–0.9 eV that we find for this surface agrees well with the activation energy for adatom diffusion that has been estimated from high-temperature scanning tunneling microscopy (STM) measurements.[74] Whether the distortion of adatom bonding is large enough to lead to the formation of a dihydride intermediate, or whether desorption occurs in a direct four-center reaction, could probably already be decided in slab calculations with a 2×2 unit cell that contains one adatom and one rest atom.

The presently discussed desorption models for H_2/Si(100) fall into two categories: Group 1 are direct one-step mechanisms. In the model already introduced above, two hydrogen atoms from doubly occupied dimers recombine and desorb through a symmetric[37] or more likely an asymmetric transition state.[30,33,35,36] These models are in agreement with the desorption kinetics, and slab calculations based on density functional theory give the experimental activation energy for the desorption.[2,6] However, the lattice distortion in the transition state is too weak at least by a factor of 2, as discussed in Sec. III for our own PES. Similar quantitative discrepancies between experimental and calculated values for translational heating and phonon-assisted sticking may be expected for the other PES's of Refs. 35, 30, and 36. In addition, the fact that the dimerization is a special feature of the Si(100) surface, whereas the energetics and dynamics of adsorption and desorption are very similar on Si(100) and Si(111), may be an argument against such a process.

Another one-step mechanism is the interdimer recombination of two hydrogen atoms from adjacent dimers on the same row.[17,30] Vittadini and Selloni[30] find that the interdimer pathway is energetically only slightly less favorable than the intradimer desorption treated by the same theory ($E_{\mathrm{des}}=2.7$ eV vs 2.5 eV). Moreover, the energy that remains in the substrate after desorption was found to be approximately equal to 0.8 eV, which is in excellent agreement with the PES of Fig. 10 and with our experimental value for phonon-assisted sticking. The significantly larger amount of lattice distortion, as compared to the interdimer recombination, arises from the large distance between the two involved silicon atoms of 3.85 Å, and its reduction by a concerted movement of Si atoms. (In case of the interdimer process a stretching of the dimer bond, which could in principle lower the adsorption barrier, instead leads to an enlargement of the distance of the reaction partners.) A problem of this model is that it does not readily explain the first-order desorption kinetics. However, clustering of adsorbed hydrogen would, e.g., lead to approximate first-order kinetics.

The second category of reaction mechanisms of H_2 with Si(100) surfaces are two-step processes with a dihydride intermediate formed at steps or single-atom defects. These defect models have been advanced by several groups,[18,21,27] because their *ab initio* cluster calculations for desorption from single dimers yielded activation energies for desorption between 3.4 and 4.1 eV (Refs. 17, 18, 20, 21, and 26) which are much higher than the 2.5 eV observed experimentally. While such an argumentation is certainly debatable in view of the much lower values for E_{des} that have recently been obtained by density-functional slab[30,33,35] and cluster calculations imposing less geometrical constraints,[36] defect-mediated processes should not readily be ruled out for the Si(100) surface.

Based on the present results we can, on the one hand, safely exclude a very basic defect model that simply explains the small sticking coefficient by a low concentration of static defects. In such a model the observed surface temperature dependence of sticking would have to arise from diffusion of atomic hydrogen from the reactive sites across the terraces. However, the measured activation energy for Si(100), $E_a\simeq0.7$ eV, is much smaller than any calculated diffusion barrier of 1.3–2.0 eV,[19,22,28] and the measured value of 1.5 eV for Si(111)7×7.[7] On the other hand, if the defects as active sites are created transiently by a thermally activated process, the mechanism becomes very similar to the model discussed in this work.

In the dihydride state, one of the normally present three Si–Si bonds is broken or at least considerably weakened, and the adsorption barrier will certainly strongly vary as a function of the Si–Si bond length x, like in our model. On perfect terraces the energy required to bring the Si lattice into a dihydridelike configuration is certainly too high. The isomerization energy between monohydride and dihydride was calculated to be 1.9 eV (Ref. 30) [compare also the Si–Si dimer bond strength of ~1.3 eV (Ref. 18)]. However, distorted dimers at steps might facilitate such excitations with energies on the order of the 0.7 eV that we find for the effective activation energy of phonon-assisted sticking. High-temperature STM measurements, e.g., show that above $T_s\simeq600$ K the steps of Si(100) become rough and move rapidly across the surface.[74] The overall activation energy for desorption from such an activated defect agrees well with the experimental value of 2.5 eV, because the activation energy for desorption from the dihydride state is known to be slightly less than 2 eV.[13]

V. CONCLUSIONS

We have presented results from a comprehensive experimental and theoretical study of the reaction dynamics of molecular hydrogen with silicon surfaces. The sticking probabilities for dissociative adsorption of H_2 and D_2 on—as well as the rates for recombinative desorption from—Si(111)7×7 and Si(100)2×1 have been determined experimentally with optical second-harmonic generation. A rather similar behavior is observed on both surfaces and for both isotopes.

At gas temperatures of 300 K, adsorption depends strongly on the surface temperature T_s and reveals phonon-

assisted sticking. In the case of Si(111)7×7, the initial sticking probabilities increase dramatically from $s_0=2\times10^{-9}$ at $T_s=580$ K to $s_0=5\times10^{-6}$ at $T_s=1050$ K. For Si(100)2×1, dissociative adsorption is slightly more probable; in the temperature range $T_s=550$–1000 K the sticking probabilities for H_2 and D_2 increase from 10^{-8} to 10^{-5}. The absolute value of desorption rates of H_2 and D_2 from both surfaces differ by less than a factor of 5 in the temperature range $T_s=700$–850 K, and reveal similar desorption barriers of 2.3–2.5 eV. On Si(111)7×7 the sticking coefficient *increases* by a factor of 3 between 0- and 0.4-ML hydrogen coverage.

From the fact that H_2 adsorption on Si(111)7×7 does not show signs of site blocking for coverages up to almost half a monolayer, we conclude that the H_2 dissociation takes place on the terraces of this surface and is not mediated by step or defect sites. The relatively small isotope effect observed for the rates of desorption and adsorption of a thermal gas suggests that tunneling plays only a minor role in the H_2 interaction with silicon surfaces. The surprisingly similar quantitative and qualitative behavior of Si(111)7×7 and Si(100)2×1 indicates that the structural details of the surface are of little importance for the energetics and dynamics of the reaction.

An effective five-dimensional model containing, in addition to the translational coordinate, one substrate degree of freedom, molecular vibrations, and surface corrugation is capable of describing *all* existing experimental data of molecular hydrogen adsorption and desorption from Si(111) and Si(100), namely, (1) the translational energy distribution of desorbing molecules (absence of translational heating), (2) the temperature dependence of the sticking coefficient as well as (3) its absolute value (preexponential), (4) the heating of molecular vibrations in desorption (including its isotope effect), and (5) the angular distribution of desorbing molecules. The model contains only very few parameters: The curvature was taken from *ab initio* calculations, and three frequencies were obtained by fitting other experimental data. One essential parameter is the barrier height for adsorption, determined so as to describe the low room-temperature sticking coefficient.

The results of the dynamical calculations are to some extent independent of the microscopic interpretation of the *substrate degree of freedom*. We have considered an *effective surface oscillator*. One should keep in mind, however, that this oscillator has to describe several degrees of freedom in an average way, and might even include nonadiabatic electronic processes. Several microscopic mechanisms that involve considerable lattice distortion in the transition state appear to be quite plausible. Attempts to establish the relationship to the dynamically relevant microscopic degrees of freedom by means of *ab initio* calculations for the H_2 interaction with the dimers of Si(100) have so far been successful only in a qualitative way. Reasons for the quantitative discrepancies from our model, as well as from the experiments, may come from inherent approximations of density-functional theory, restrictions to small unit cells or clusters, or difficulties in finding the energetically most favorable reaction path on relatively complex surfaces.

ACKNOWLEDGMENTS

The authors would like to thank K. L. Kompa, J. Nørskov, and M. Scheffler for valuable discussions. This research was supported by the Deutsche Forschungsgemeinschaft through Sonderforschungsbereich 338 (Project Nos. C2 and C5), by the EEC Human Capital Programme (No. CHRX-CT93-0104), and by the Danish National Research Foundation.

[1] K. Sinniah, M. G. Sherman, L. B. Lewis, W. H. Weinberg, J. T. Yates, Jr., and K. C. Janda, Phys. Rev. Lett. **62**, 567 (1989); J. Chem. Phys. **92**, 5700 (1990).

[2] M. L. Wise, B. G. Koehler, P. Gupta, P. A. Coon, and S. M. George, Surf. Sci. **258**, 166 (1991).

[3] J. J. Boland, Phys. Rev. Lett. **67**, 1539 (1991); J. Vac. Sci. Technol. A **10**, 2458 (1992).

[4] G. A. Reider, U. Höfer, and T. F. Heinz, J. Chem. Phys. **94**, 4080 (1991).

[5] G. A. Reider, U. Höfer, and T. F. Heinz, Phys. Rev. Lett. **66**, 1994 (1991).

[6] U. Höfer, L. Li, and T. F. Heinz, Phys. Rev. B **45**, 9485 (1992).

[7] P. Bratu and U. Höfer, Phys. Rev. Lett. **74**, 1625 (1995).

[8] P. Bratu, K. L. Kompa, and U. Höfer, Chem. Phys. Lett. **251** 1 (1996).

[9] K. W. Kolasinski, S. F. Shane, and R. N. Zare, J. Chem. Phys. **96**, 3995 (1992); S. F. Shane, K. W. Kolasinski, and R. N. Zare, *ibid.* **97**, 3704 (1992).

[10] S. F. Shane, K. W. Kolasinski, and R. N. Zare, J. Chem. Phys. **97**, 1520 (1992).

[11] K. W. Kolasinski, W. Nessler, A. de Meijere, and E. Hasselbrink, Phys. Rev. Lett. **72**, 1356 (1994).

[12] K. W. Kolasinski, W. Nessler, K.-H. Bornscheuer, and E. Hasselbrink, J. Chem. Phys. **101**, 7082 (1994); Surf. Sci. **331-333**, 485 (1995).

[13] M. C. Flowers, N. B. H. Jonathan, Y. Liu, and A. Morris, J. Chem. Phys. **99**, 7038 (1993).

[14] Y-S. Park, J-S. Bang, and J. Lee, Surf. Sci. **283**, 209 (1993); Y.-S. Park, J.-Y. Kim, and J. Lee, J. Chem. Phys. **98**, 757 (1993).

[15] W. Widdra, S. I. Yi, R. Maboudian, G. A. D. Briggs, and W. H. Weinberg, Phys. Rev. Lett. **74**, 2074 (1995).

[16] Y. Morita, K. Miki, and H. Tokumoto, Surf. Sci. **325**, 21 (1995).

[17] C. J. Wu and E. A. Carter, Chem. Phys. Lett. **185**, 172 (1991).

[18] C. J. Wu, I. V. Ionova, and E. A. Carter, Surf. Sci. **295**, 64 (1993).

[19] C. J. Wu, I. V. Ionova, and E. A. Carter, Phys. Rev. B **49**, 13 488 (1994).

[20] P. Nachtigall, K. D. Jordan, and K. C. Janda, J. Chem. Phys. **96**, 852 (1991).

[21] P. Nachtigall, K. D. Jordan, and C. Sosa, J. Chem. Phys. **101**, 8073 (1994).

[22] P. Nachtigall and K. D. Jordan, J. Chem. Phys. **102**, 8349 (1995).

[23] M. P. D'Evelyn, Y. L. Yang, and L. F. Suctu, J. Chem. Phys. **96**, 852 (1992); Y. L. Yang and M. P. D'Evelyn, J. Vac. Sci. Technol. A **11**, 2200 (1993).

[24] J. Sheng and J. Z. H. Zhang, J. Chem. Phys. **97**, 596 (1992).

[25] Z. Jing and J. L. Whitten, Phys. Rev. B **46**, 9544 (1992).
[26] Z. Jing and J. L. Whitten, J. Chem. Phys. **98**, 7466 (1993); **102**, 3867 (1995).
[27] Z. Jing, G. Lucovsky, and J. L. Whitten, Surf. Sci. Lett. **296**, L33 (1993).
[28] A. Vittadini, A. Selloni, and M. Casarin, Surf. Sci. **289**, L625 (1993).
[29] A. Vittadini, A. Selloni, and M. Casarin, Phys. Rev. B. **49**, 11 191 (1994).
[30] A. Vittadini and A. Selloni, Chem. Phys. Lett. **235**, 334 (1995).
[31] W. Brenig, A. Groß, and R. Russ, Z. Phys. B **96**, 231 (1994).
[32] D. C. Sorescu, D. L. Thompson, and L. M. Raff, J. Chem. Phys. **101**, 1638 (1994).
[33] P. Kratzer, B. Hammer, and J. K. Nøskov, Chem. Phys. Lett. **229**, 645 (1994); Phys. Rev. B **51**, 13 432 (1995).
[34] P. Kratzer, R. Russ, and W. Brenig, Surf. Sci. **345**, 125 (1996).
[35] E. Pehlke and M. Scheffler, Phys. Rev. Lett. **74**, 952 (1995).
[36] S. Pai and D. Doren, J. Chem. Phys. **103**, 1232 (1995).
[37] Guangwei Li, Yia-Chung Chang, R. Tsu, and J. E. Greene, Surf. Sci. **330**, 20 (1995).
[38] J. M. Jasinski, B. S. Meyerson, and B. A. Scott, Annu. Rev. Phys. Chem. **38**, 109 (1987).
[39] W. Kern, Semicond. Int. **7**, 94 (1984); E. Yablonovitch, D. L. Allara, C. C. Chang, T. Gmitter, and T. B. Bright, Phys. Rev. Lett. **57**, 249 (1986); G. S. Higashi, Y. J. Chabal, G. W. Trucks, and K. Raghavachari, Appl. Phys. Lett. **56**, 656 (1990).
[40] J. T. Law, J. Chem. Phys. **30**, 1568 (1959).
[41] G. Schulze and M. Henzler, Surf. Sci. **124**, 336 (1983).
[42] M. Liehr, C. M. Greenlief, M. Offenberg, and S. R. Kasi, J. Vac. Sci. Technol. A **8**, 2960 (1990).
[43] *Proceedings of the International Workshop on Surface Reconstruction: Structure and Dynamics*, Erlangen, Germany, 1994, edited by R. J. Behm and K. Heinz [Surf. Sci. **337**, 169 (1995)].
[44] U. Bischler, P. Sandl, E. Bertel, T. Brunner, and W. Brenig, Phys. Rev. Lett. **70**, 3603 (1993).
[45] J. C. Polanyi and W. H. Wong, J. Chem. Phys. **51**, 1439 (1969).
[46] U. Höfer, G. A. Ratzlaff, Leping Li, and T. F. Heinz, Phys. Rev. B **52**, 5264 (1995).
[47] T. F. Heinz, in *Nonlinear Surface Electromagnetic Phenomena*, edited by H.-E. Ponath and G. I. Stegeman (North-Holland, Amsterdam, 1991), p. 353.
[48] U. Höfer, *Proceedings, Symposium on Surface Science 3S'95*, edited by P. Varga and G. Betz (Tu Wien, Vienna, 1995), pp. 3–10; G. A. Schmitt and U. Höfer (unpublished).
[49] F. J. Himpsel, Surf. Sci. Rep. **12**, 1 (1990).
[50] K. Takayanagi, Y. Tanishiro, S. Takahashi, and M. Takahashi, Surf. Sci. **164**, 367 (1985).
[51] G. L. Hofacker, Z. Naturforschung **18a**, 607 (1963).
[52] W. Brenig and H. Kasai, Surf. Sci. **213**, 170 (1989).
[53] W. Brenig and R. Russ, Surf. Sci. **315**, 195 (1994).
[54] W. Brenig, A. Groß, and R. Russ, Z. Phys. B **97**, 311 (1995).
[55] D. C. Allan and E.J. Mele, Phys. Rev. Lett. **53**, 826 (1984).
[56] H. Bilz and W. Kress, *Phonon Dispersion Relations in Insulators* (Springer, Berlin, 1978).
[57] A. Groß, B. Hammer, M. Scheffler, and W. Brenig, Phys. Rev. Lett. **73**, 3121 (1994).
[58] A. Groß, J. Chem. Phys. **102**, 5045 (1995).
[59] G. R. Darling and S. Holloway, Surf. Sci. **304**, L461 (1994).
[60] J. A. Schaefer, F. Stucki, J. A. Anderson, G. J. Lapeyre, and W. Göpel, Surf. Sci. **140**, 207 (1984).
[61] H. Froitzheim, U. Köhler, and H. Lammering, Surf. Sci. **149**, 537 (1985).
[62] W. Brenig, T. Brunner, A. Groß, and R. Russ, Z. Phys. B **93**, 91 (1993).
[63] C. C. Rankin and J. C. Light, J. Chem. Phys. **51**, 1701 (1969).
[64] J. Harris, S. Holloway, T. S. Rahman, and K. Yang, J. Chem. Phys. **89**, 4427 (1988).
[65] S. Küchenhoff, W. Brenig, and Y. Chiba, Surf. Sci. **245**, 389 (1991).
[66] Y. J. Chabal and K. Raghavachari, Phys. Rev. Lett. **53**, 282 (1984); **54**, 1055 (1985).
[67] J. Dabrowski and M. Scheffler, Appl. Surf. Sci. **56-58**, 15 (1992).
[68] R. A. Wolkow, Phys. Rev. Lett. **68**, 2636 (1994).
[69] E. L. Bullock, R. Gunella, L. Patthey, T. Abukawa, S. Kono. C. R. Natoli, and L. S. O. Johansson, Phys. Rev. Lett. **74**, 2756 (1995).
[70] P. Krüger, A. Mazur, J. Pollmann, and G. Wolfgarten, Phys. Rev. Lett. **57**, 1468 (1986).
[71] P. Nachtigall, K. D. Jordan, A. Smith, and H. Jónsson, J. Chem. Phys. **104**, 148 (1996).
[72] A. C. Luntz and P. Kratzer, J. Chem. Phys. **104**, 3075 (1996).
[73] A. Vittadini and A. Selloni, Phys. Rev. Lett. **75**, 4756 (1995).
[74] H. Tokumoto and M. Iwatsuki, Jpn. J. Appl. Phys. **32**, 1368 (1993).